Light source engineering of directive photoluminescent metasurfaces with the local Kirchhoffs law

Elise Bailly, Jean Paul Hugonin, B. Vest, Jean-Jacques Greffet

Light source engineering of directive photoluminescent metasurfaces with the local Kirchhoffs law

*Elise Bailly Jean-Paul Hugonin Jean-René Coudevylle Corentin Dabard Sandrine Ithurria Benjamin Vest Jean-Jacques Greffet**

E. Bailly, J.-P. Hugonin, B. Vest, J.-J. Greffet
Université Paris-Saclay, Institut d'Optique Graduate School, CNRS, Laboratoire Charles Fabry, 91120 Palaiseau, France
Email Address: jean-jacques.greffet@institutoptique.fr
J.-R. Coudevylle
Centre de Nanosciences et de Nanotechnologies, Université Paris-Saclay, CNRS, 91120 Palaiseau, France
C. Dabard, S. Ithurria
Laboratoire de Physique et d'Etude des Matériaux, ESPCI-Paris, PSL Research University, Sorbonne Université UPMC Univ Paris 06, CNRS, 10 Rue Vauquelin, 75005 Paris, France

Keywords: *metasurfaces, photoluminescence, directionality, Kirchhoff*

1 Nanoplatelets' properties

1.1 Emission and Absorption spectra of the nanoplatelets

The absorption and emission spectra of the nanoplatelets (NPLs) (in solution in hexane) are given in Figure 1. The peak emission wavelength is 605 nm. The Stokes shift, evaluated between the absorption peak (blue dotted line) and the emission peak (red dotted line) is 20 nm.

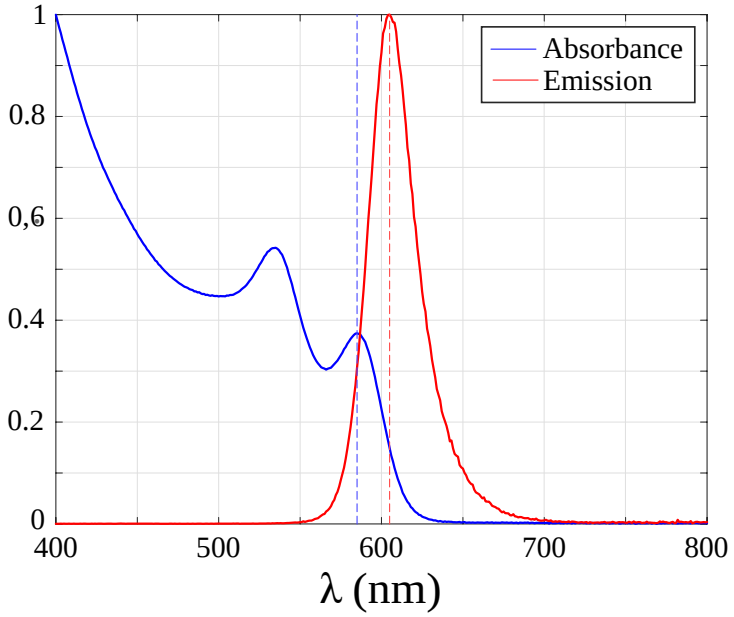

Figure 1: Normalized emission and absorption spectra of the solution of NPLs in hexane in arbitrary units.

1.2 TEM images

The TEM (transmission electron microscopy) image of the NPLs is presented in Figure 2. For TEM imaging, a drop of diluted NPLs solution in hexane is drop-casted on a copper grid covered with an amorphous carbon film. The grid is degassed overnight under secondary vacuum. A JEOL 2010F is used at 200 kV for the picture acquisition.

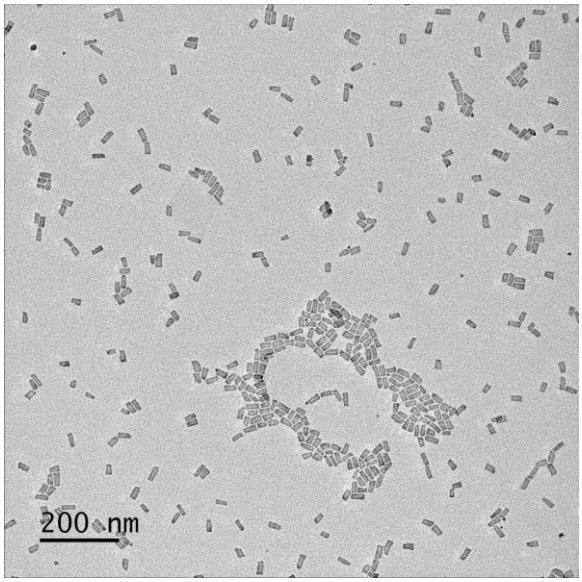

Figure 2: TEM image of the NPLs.

1.3 Refractive index of the nanoplatelets

In order to measure the refractive index of the NPLs, we fabricated a sample consisting on NPLs deposited by spin coating on top of a stack 50 nm thick layer of silver/ 1 nm thick layer of germanium/ SF10 glass substrate. Silver and germanium were deposited using electron beam evaporation. To deposit the NPLs, 200 µL of a NPLs solution was spin coated on the metallic substrate at 500 rpm during 30 seconds with an acceleration ramp of 5 seconds. The ellipsometry measurements were performed in three steps.

1. First, the refractive index of a SF10 glass substrate was measured to serve as a reference.
2. The refractive index of silver (including 1 nm of germanium) was measured from a reference sample which was fabricated under the same conditions as the sample covered with NPLs. It thus consists in a 50 nm thick layer of silver on a 1 nm thick layer of germanium, on a SF10 glass substrate. The experimental refractive index is similar to the silver index of reference [1], as it can be seen in Figure 3, so that the germanium layer has little impact on the refractive index. The thickness of the layer was obtained by scratching it with a needle and measuring the depth of the slit by AFM. We obtained 50 ± 3 nm, in agreement with the nominal value.
3. Knowing the refractive index models of glass and silver, the refractive index of the NPLs was extracted from ellipsometry data and processed using a B-spline method (which is Kramers-Kronig consistent). The refractive index is given in Figure 4. The total thickness of the sample was obtained by scratching it with a needle and measuring the total depth of the slit by AFM. By substracting the experimental thickness values of the silver and germanium layers obtained from the reference sample, we obtained 42 ± 5 nm thick.

In order to perform the dispersion relation computed with a complex frequency presented in Figure 5 in the main article [2], we fitted the index of the NPLs as well as the index of silver by a polynomial of degree 2: $p(\lambda) = p_1\lambda^n + p_2\lambda^{n-1} + ... + p_n\lambda + p_{n+1}$, with the Matlab® function "polyfit". The fitting coefficients are given in Table 1. The comparisons between the ellipsometry measurements and the polynomial fits are presented in Figure 3 for the silver and in Figure 4 for the NPLs. A higher degree of the polynomial fits more accurately the experimental data, but the dispersion relation remains the same.
Nevertheless, the absorptivity computations presented in the main article [2] are done with an interpollation of experimental index of the NPLs obtained by ellipsometry and the refractive index of silver of reference [1].

	NPLs	Ag
p_1	$0.5186 + 0.3912i$	$1.0159 - 3.7984i$
p_2	$-0.9402 - 0.7008i$	$-1.2376 + 12.7632i$
p_3	$2.1514 + 0.3220i$	$0.5036 - 2.5394i$

Table 1: Coefficients for the polynomial fit $p(\lambda) = p_1\lambda^n + p_2\lambda^{n-1} + ... + p_n\lambda + p_{n+1}$, of degree $n = 2$ of the refractive index of the nanoplatelets (NPLs) of Figure 4 and the refractive index of silver (Ag) of Figure 3.

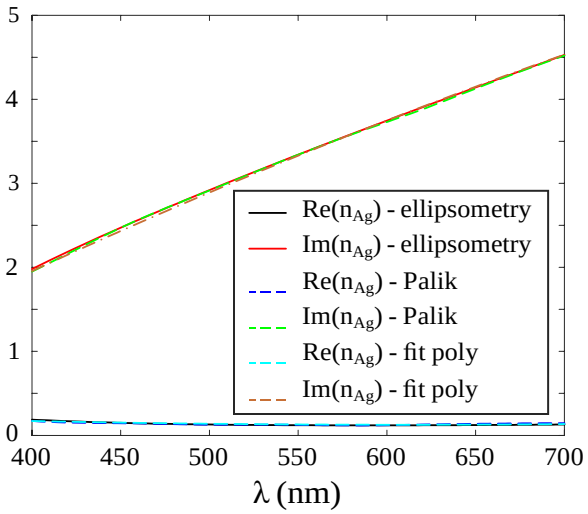

Figure 3: Refractive index of silver, measured by ellipsometry from a sample composed of 50 nm of silver on top of a 1 nm of Germanium on a SF10 glass substrate. The experimental values are compared with the refractive index of silver of reference [1], named "Palik" and the polynomial fit whose coefficients are given in Table 1.

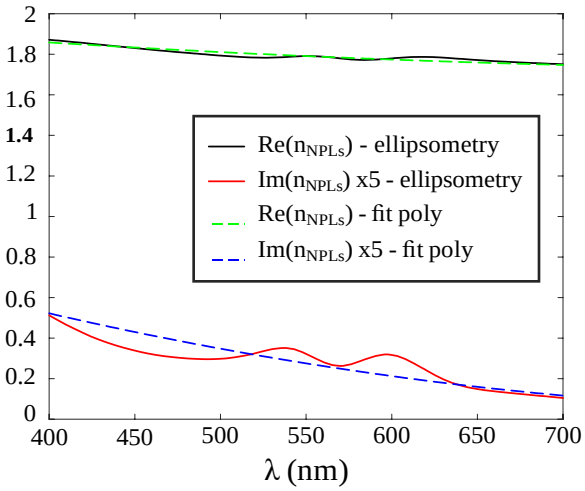

Figure 4: Refractive index of the NPLs measured by ellipsometry and comparison with the polynomial fit whose coefficients are given in Table 1, from a sample composed of 42±5 nm thick layer of NPLs deposited by spin coating on top of a 50 nm of silver on a 1 nm of Germanium, on a SF10 glass substrate. For the sake of clarity, the imaginary part of the refractive index is multiplied by 5.

2 Spatial structure of the surface plasmon

This section shows the spatial structure of the mode which exists at the interface between a silver substrate and a thin layer (2 nm) of NPLs at 607.4 nm, computed with the refractive index of the NPLs measured by ellipsometry and the refractive index of silver of reference [1]. Figure 5 shows that the mode is evanescent both in metal and in air. It corresponds to a surface plasmon polariton at the interface metal/NPLs/air.

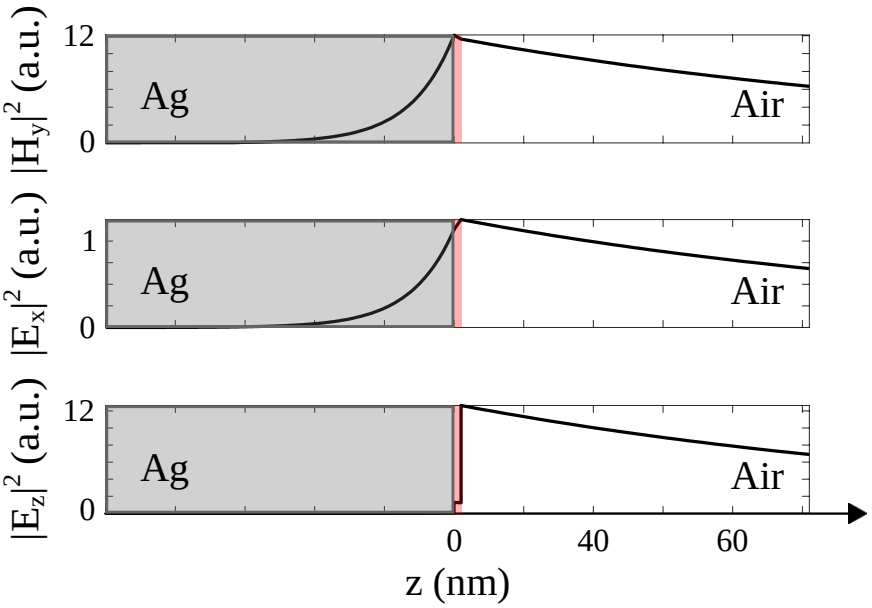

Figure 5: Spatial structure of the mode as a function of z at 607.4 nm (in arbitrary units), for a sample composed of 2 nm thick layer of NPLs (in pink hue area) on silver. At this wavelength the refractive indexes are $n_{NPLs} = 1.7844 + 0.0598i$, $n_{Ag} = 0.1260 + 3.7852i$ and $n_{eff} = 1.0419 + 0.0031i$.

3 Estimation of the beam efficiency

In this section, we present the computation of the beam efficiency at the experimental peak emission wavelength (at 607.4 nm), defined as P_{lobe}/P_{tot}, where $P_{lobe} = \int_0^{k_{lobe}} dP_e$ is the emitted power in the emission peak represented in red in Figure 6, with $k_{lobe} = 2.40\ \mu m^{-1}$.
Since the signal is symmetrical in $\pm k_x$, we integrate over the positive axis only and multiply by two.
The total power P_{tot} has been determined in two different ways:

- Experimentally, light is collected within a light cone limited by the numerical aperture of the objective (NA = 0.75), so that it is not possible to obtain the exact total power emitted between 0° and 90°. However, it is possible to estimate the beam efficiency with the total power collected, called $P_{tot}^{min} = \int_0^{k_{min}} dP_e$, represented with green dotted lines in Figure 6. We chose a value of $k_{min} = 7.36\ \mu m^{-1}$ (corresponding to 45.3° at 607.4 nm), slightly lower than $k_{NA} = k_0 NA$, before the signal decreases (see Fig. 6). This estimation gives an overestimation of the beam efficiency value. We obtain a beam efficiency of 44.8 %.

- It is also possible to give a boundary value of the total emitted power emitted between 0 and 90°, by extrapolating the value of the emitted power at k_{min} for $k > k_{min}$. The integrated power is then $P_{tot}^{max} = \int_0^{k_{max}} dP_e$ and is represented with blue dotted lines in Figure 6. Thus, we obtain an underestimation of the beam efficiency value of 35 %.

We therefore estimate that the radiative efficiency lies in the range 35% and 44.8 %.

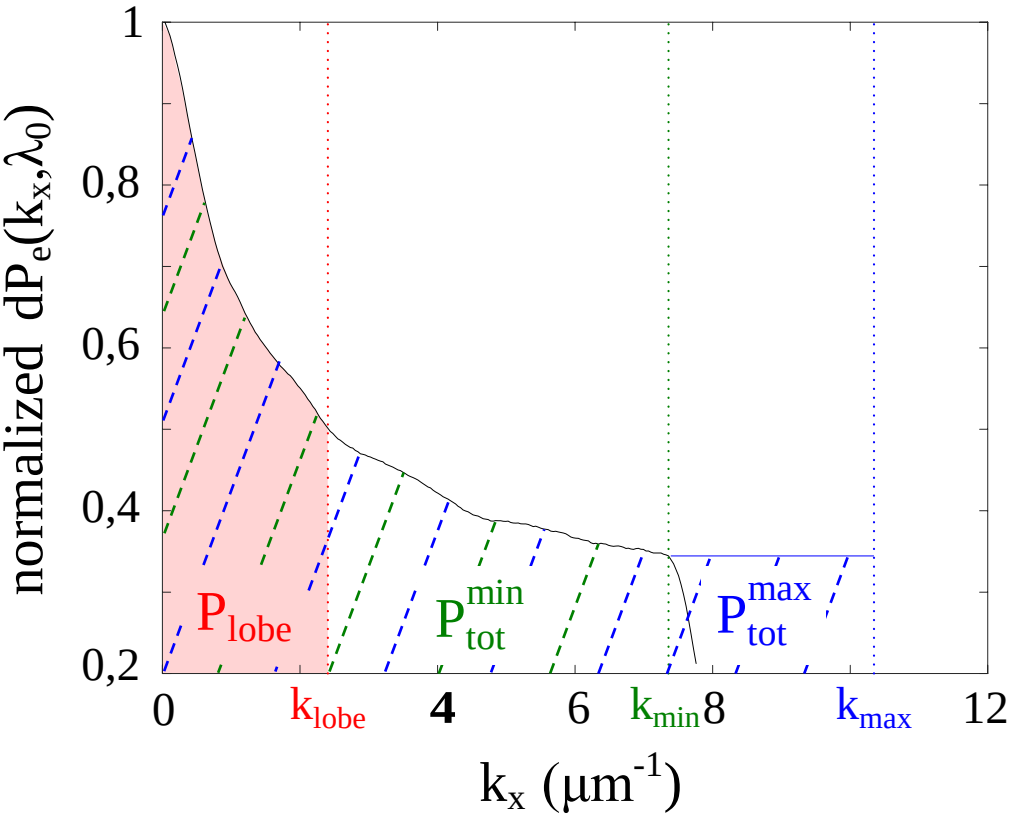

Figure 6: Normalized experimental emitted power density as a function of k_x at the peak emission wavelength, for the 2D silver metasurface covered with NPLs. Three emitted power values, each defined by different wavevector integration boundaries, can be computed: $P_{lobe} = \int_0^{k_{lobe}} dP_e$, $P_{tot}^{min} = \int_0^{k_{min}} dP_e$, $P_{tot}^{max} = \int_0^{k_{max}} dP_e$ with $k_{lobe} = 2.40\ \mu m^{-1}$, $k_{min} = 7.36\ \mu m^{-1}$ and $k_{max} = 10.35\ \mu m^{-1}$.

4 Emission and Absorption for TE and TM polarization states

We present in Figure 7 the comparisons between normalized experimental radiation patterns and the normalized absorptivities, for Transverse Electric (TE), Transverse Magnetic (TM) polarization states, and for the total emitted power, plotted at their experimental peak emission wavelengths. Only the last case is presented in the article [2].

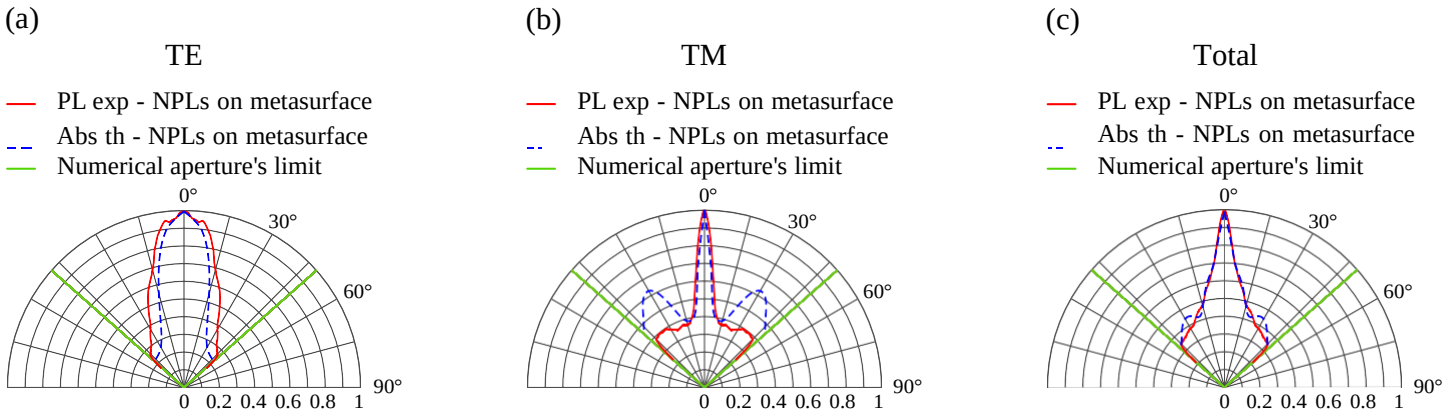

Figure 7: Normalized experimental radiation patterns at their peak emission wavelengths (red curve) and normalized theoretical absorption pattern calculated at the same peak emission wavelengths (blue dotted line), as a function of the polarization state (a): Transverse Electric (TE) at 608.4 nm, (b): Transverse Magnetic (TM) at 605.8 nm, (c): Total emission at 607.4 nm, for h_{res} = 100 nm, l_{res} = 450 nm, p_{res} = 600 nm, $h_{top-NPLs}$ = 2 nm.

We also present in Figure 8 the comparison between the experimental radiation patterns and the normalized absorptivities for $h_{top-NPLs}$ = 0 nm, that is considering there was no overfilling of the grating grooves, and showing a less good agreement.

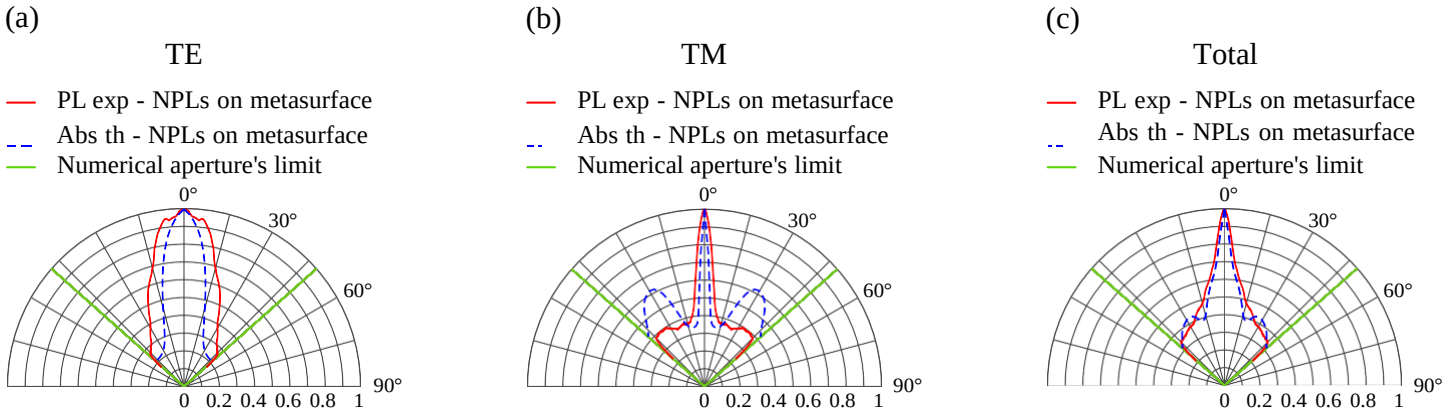

Figure 8: Normalized experimental radiation patterns at their peak emission wavelengths (red curve) and normalized theoretical absorption pattern calculated at the same peak emission wavelengths (blue dotted line), as a function of the polarization state (a): Transverse Electric (TE) at 608.4 nm, (b): Transverse Magnetic (TM) at 605.8 nm, (c): Total emission at 607.4 nm, for h_{res} = 100 nm, l_{res} = 450 nm, p_{res} = 600 nm, $h_{top-NPLs}$ = 0 nm.

References

[1] E. Palik, *Handbook of Optical Constants of Solids: Volume 1*. No. vol. 1, Elsevier Science, 2012.

[2] See Article.